Journal of Molecular Graphics and Modelling 27 (2008) 326–331

Contents lists available at ScienceDirect

Journal of Molecular Graphics and Modelling

journal homepage: www.elsevier.com/locate/JMGM

Theoretical ^{14}N nuclear quadrupole resonance parameters for sulfa drugs: Sulfamerazine and sulfathiazole

Mehdi D. Esrafili, Hadi Behzadi, Javad Beheshtian, Nasser L. Hadipour *

Department of Chemistry, Tarbiat Modares University, P.O. Box: 14115-175, Tehran, Iran

ARTICLE INFO

Article history:
Received 3 March 2008
Received in revised form 25 May 2008
Accepted 27 May 2008
Available online 5 June 2008

Keywords:
Electric field gradient tensor
Atoms in Molecules (AIM) analysis
Nuclear quadrupole coupling constant
Sulfamerazine
Sulfathiazole

ABSTRACT

A density functional theory investigation was carried out to characterize ^{14}N electric field gradient tensors, EFG, in crystalline sulfamerazine and sulfathiazole. To include hydrogen-bonding effects in the calculations, the most probable interacting molecules with the target were considered as tetrameric and pentameric clusters, respectively. The calculated EFG tensors were used to evaluate nuclear quadrupole coupling tensors (χ_{ii}) and asymmetry parameters (η_Q) for the target molecule in the clusters. Results are in satisfactory agreement with the experimental data. The EFG calculations reveal different contributions of nitrogen atoms in hydrogen-bonding network of the sulfamerazine and sulfathiazole. Moreover, based on the results obtained via atoms in molecules (AIM) analyses, an acceptable linear relation between ^{14}N nuclear quadrupole coupling constants and charge density values at N–H···N and N–H···O bond critical points, $\rho_b(\mathbf{r}_{cp})$, is observed.

1. Introduction

Along with oxygen, carbon, and hydrogen, nitrogen atom constitutes the most essential element in chemistry of biomolecules and many inorganic compounds related to material sciences. It plays a key role in the formation of polypeptide backbone, side-chain conformation and hydrogen-bonding (H-bonding) interactions in biosystems [1]. These effects and interactions may be thoroughly studied via techniques which can probe the chemical environment of nitrogen sites. Nuclear quadrupole resonance (NQR) spectroscopy is well recognized as an insightful technique to characterize the nature of intermolecular interaction and molecular structure in solid-phase [2–9]. Nuclei with spin angular momentum, I, greater than one-half ($I > 1/2$), have electric quadrupole moment, eQ, which interacts with electric field gradient tensor, EFG. The quadrupole coupling constant, QCC, calculated from NQR frequency, is proportional to charge on quadrupole nuclei and gives information on electron distribution in a molecule, whereas asymmetry parameter, η_Q, provides information on the direction and order of chemical bonds [10].

Sulfonamides drugs exhibit interesting solid-state properties, and can form various H-bonding interactions in crystalline structures [11–13]. Some bioactivities have been detected for aromatic sulfonamides: antiangiogenic [14,15], antitumor [16], anti-inflammatory and anti-analgestic [17]. sulfamerazine ($C_{11}H_{12}N_4O_2S$) and sulfathiazole ($C_9H_9N_3O_2S_2$) are two well-known and widely used members of sulfonamides. Numerous experimental techniques including X-ray and neutron diffraction crystallography, infrared, Raman and nuclear magnetic resonance, NMR, spectroscopies have been applied to characterize the nature of H-bonding interactions for sulfonamides and their derivatives in solid-phase [18–24]. Adsmond and Grant [25] investigated the nature of H-bonding interactions in 39 sulfonamide crystalline structures. They indicated a greater preference of amide proton for H-bonding to amidine nitrogens in sulfonamides. Recent work by Hossain [18] presented the capability of sulfamerazine to construct a hydrogen-bonded lattice through the N–H···O and N–H···N interactions in the solid-phase. Blinc et al. [26] experimentally measured the ^{14}N nuclear quadrupole coupling constants and asymmetry parameters of sulfamerazine and sulfathiazole. Their work indicated the importance of intermolecular H-bonding interactions in assigning the ^{14}N quadrupole coupling constants and asymmetry parameters for sulfa drugs.

Previous studies demonstrate the reproduction quality and reliability of calculated EFG tensors and NQR parameters obtained from real crystalline structures [27,8,28]. Jakobsen and co-workers [9] indicated that structure refinement of RbNO3 and CsNO3 XRD crystal structures can actually be possible by coupling of precisely

* Corresponding author. Tel.: +98 2188011001 3495; fax: +98 218800 9730.
E-mail address: hadipour@modares.ac.ir (N.L. Hadipour).

1093-3263/$ – see front matter © 2008 Elsevier Inc. All rights reserved.
doi:10.1016/j.jmgm.2008.05.007

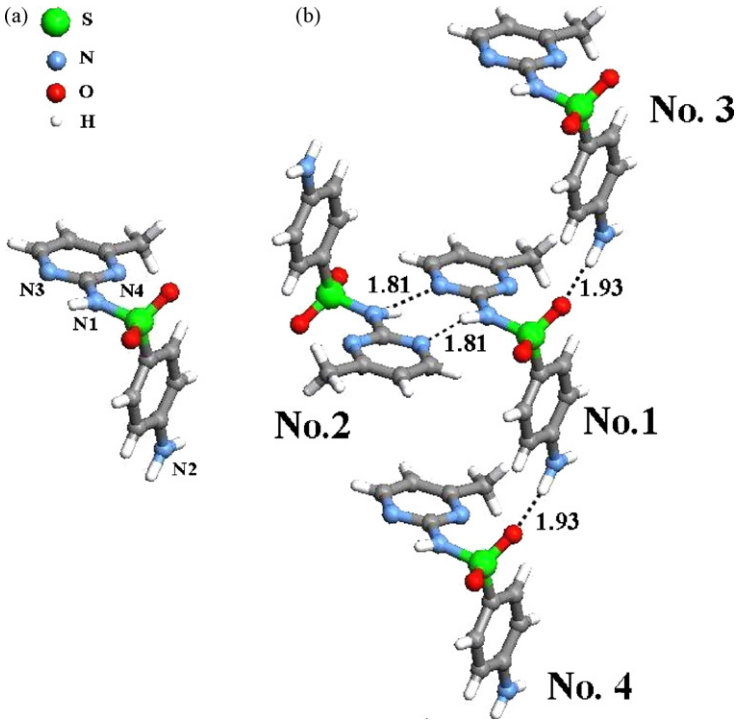

Fig. 1. (a) Monomer and (b) H-bonded network of crystalline sulfamerazine. The target molecule (No. 1): (x, y, z); No. 2: $(1-x, -y, 1-z)$; No. 3: $(1-x, -1-y, 1-z)$; No. 4: $(-1-x, 1-y, 1-z)$.

determined QCC(^{14}N) and η_Q(^{14}N) with density functional theory (DFT) calculations. In this work, ^{14}N EFG tensors of crystalline sulfamerazine and sulfathiazole are evaluated by DFT calculations. Therefore, due to the presence of hydrogen bonds (N–H···O and N–H···N), tetrameric and pentameric clusters are found to include the most probable interacting molecules with the target in crystalline lattice of sulfamerazine and sulfathiazole, respectively (Figs. 1 and 2). To investigate the H-bonding interactions in crystalline phase, EFG tensors were calculated for both isolated gas-phase and target molecule in the clusters. The calculated EFG tensors were used to evaluate nuclear quadrupole coupling tensors and associated asymmetry parameters (Tables 1 and 2). To rationalize the observed trends of calculated EFG tensors, target sulfamerazine and sulfathiazole wave functions were analyzed through atoms in molecules analysis, AIM (Tables 3 and 4).

Table 1
Calculated ^{14}N quadrupole coupling components (in MHz) and asymmetry parameters of sulfamerazine

Model	Nucleus	Basis set	χ_{xx}	χ_{yy}	χ_{zz} (QCC)	η_Q
Monomer	N1	6-311++G (d,p)	−2.26	−2.60	4.86	0.07
	–	6-311+G (d)	−2.35	−2.95	5.31	0.11
	N2	6-311++G (d,p)	−1.69	−2.74	4.43	0.24
	–	6-311+G (d)	−1.74	−2.84	4.62	0.24
	N3	6-311++G (d,p)	−1.98	−2.21	4.19	0.05
	–	6-311+G (d)	−2.27	−2.34	4.60	0.02
	N4	6-311++G (d,p)	−1.95	−2.47	4.42	0.12
	–	6-311+G (d)	−2.06	−2.58	4.64	0.08
Tetramer cluster	N1	6-311++G (d,p)	−1.08	−2.28	3.36	0.36
	–	6-311+G (d)	−1.16	−2.73	3.90	0.40
	N2	6-311++G (d,p)	−1.02	−2.87	3.89	0.48
	–	6-311+G (d)	−1.15	−2.96	4.11	0.44
	N3	6-311++G (d,p)	−1.47	−2.24	3.71	0.21
	–	6-311+G (d)	−1.67	−2.10	3.77	0.11
	N4	6-311++G (d,p)	−2.06	−2.17	4.23	0.03
	–	6-311+G (d)	−2.08	−2.30	4.38	0.05
Exp.[a]	N1	–	−1.27	−2.40	3.67	0.31
	N2	–	−1.03	−2.92	3.95	0.48

[a] Experimental values at 295 K from Ref. [26].

Table 2
Calculated ^{14}N quadrupole coupling components (in MHz) and asymmetry parameters of sulfathiazole

Model	Nucleus	Basis set	χ_{xx}	χ_{yy}	χ_{zz} (QCC)	η_Q
Monomer	N1	6-311++G (d,p)	1.48	2.90	−4.38	0.32
	–	6-311+G (d)	1.60	2.95	−4.55	0.28
	N2	6-311++G (d,p)	−2.59	−3.17	5.76	0.06
	–	6-311+G (d)	−2.69	−3.27	6.06	0.10
	N3	6-311++G (d,p)	−0.91	−2.40	3.32	0.45
	–	6-311+G (d)	−1.01	−2.35	3.36	0.40
Pentamer cluster	N1	6-311++G (d,p)	1.50	2.44	−3.94	0.24
	–	6-311+G (d)	1.61	2.59	−4.19	0.23
	N2	6-311++G (d,p)	−1.41	−2.56	3.77	0.30
	–	6-311+G (d)	−1.81	−2.56	4.36	0.17
	N3	6-311++G (d,p)	−0.43	−2.02	2.46	0.65
	–	6-311+G (d)	−0.59	−2.37	2.97	0.80
Exp.[a]	N1	–	1.42	2.46	−3.88	0.27
	N2	–	−1.22	−2.42	3.64	0.33
	N3	–	−0.47	−1.82	2.29	0.59

[a] Experimental values at 233 K from Ref. [26].

Table 3
BCP properties for N–H···N and N–H···O interactions in crystalline sulfamerazine[a,b]

Donor···Acceptor	Type	λ_1	λ_2	λ_3	$\rho_b(\mathbf{r}_{cp})$	$\nabla^2_\rho(\mathbf{r}_{CP})$	ε
No.1···No.2	H···N	−0.0521	−0.0485	0.1975	0.0344	0.0967	0.069
No.2···No.1	H···N	−0.0511	−0.0478	0.1999	0.0339	0.1011	0.066
No.3···No.1	H···O	−0.0288	−0.0282	0.1489	0.0153	0.0919	0.022
No.4···No.1	H···O	−0.0291	−0.0279	0.1481	0.0145	0.0909	0.041

All λ_i, $\rho_b(\mathbf{r}_{cp})$, $\nabla^2_\rho(\mathbf{r}_{CP})$ values in atomic unit. See Fig. 1 for details.

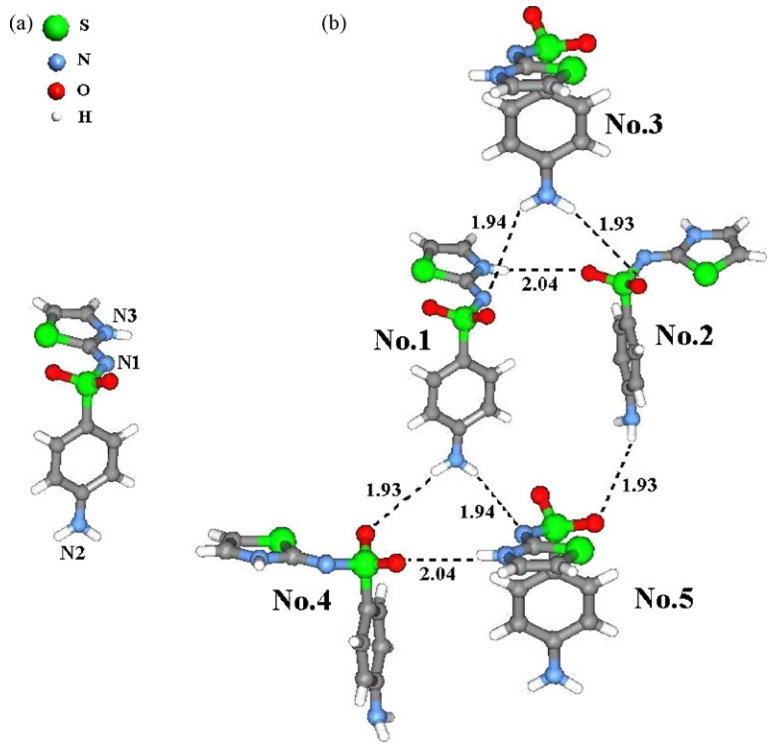

Fig. 2. (a) Monomer and (b) H-bonded network of crystalline sulfathiazole. The target molecule (No. 1): (x, y, z); No. 2: ($0.5 + x$, $0.5 - y$, $0.5 + z$); No. 3: ($1 - x$, $1 - y$, $-z$); No. 4: ($0.5 - x$, $-0.5 + y$, $0.5 - z$) and No. 5: ($1 - x$, $-$y, $-z$).

2. Computational aspects

2.1. DFT calculations

The quantum chemical calculations were carried out within the Gaussian 98 suite of package [29]. All EFG calculations were performed at DFT level with B3LYP functional using 6-311+G(d) and 6-311++G(d,p) basis sets [30–31]. The crystalline structures of sulfamerazine and sulfathiazole were adopted from X-ray diffraction data [18,32]. Since the positions of hydrogen atoms are not located accurately by X-ray diffraction, a geometry optimization of the just hydrogen atoms in the structure was needed. The optimization was performed at the B3LYP/6-31++G(d,p) level, where during this optimization the positions of the hydrogen atoms were allowed to fully relax while those of all other atoms remained frozen. For sulfamerazine and sulfathiazole crystalline structures, tetramer and pentamer clusters involving the most probable interacting molecules with the central molecule were created using coordinates transformation and were considered in the calculations, respectively (Figs. 1 and 2).

The principal components of EFG tensor, q_{ii}, are computed in atomic unit (1 au = 9.717365×10^{21} V m^{-2}), with $|q_{zz}| \geq |q_{yy}| \geq \{q_{xx}|$ and $q_{xx} + q_{yy} + q_{zz} = 0$. These diagonal elements correlate through asymmetry parameter: $\eta_Q = |(q_{yy} - q_{xx})/q_{zz}|$ and $0 \leq \eta_Q \leq 1$, that measures the deviation of EFG tensor from axial symmetry [2]. The computed q_{ii} components of EFG tensor are used to obtain the nuclear quadrupole coupling components, χ_{ii}(MHz) = e^2Qq_{ii}/h, and nuclear quadrupole coupling constant, QCC (MHz) = e^2Qq_{zz}/h, where the standard value of eQ(^{14}N) reported by Pyykkö is employed [33]: eQ(^{14}N) = 20.44 mb.

Table 4
BCP properties for N–H···N and N–H···O interactions in crystalline sulfathiazole

Donor···Acceptor	Type	λ_1	λ_2	λ_3	$\rho_b(\mathbf{r}_{cp})$	$\nabla^2_\rho(\mathbf{r}_{CP})$	ε
No.1···No.2	H···O	−0.0351	−0.0324	0.1534	0.0291	0.0849	0.083
No.3···No.1	H···N	−0.033	−0.0323	0.1400	0.0192	0.0747	0.021
No.3···No.2	H···O	−0.0301	−0.0299	0.1363	0.0217	0.0763	0.008
No.1···No.4	H···O	−0.0289	−0.0285	0.1257	0.0199	0.0683	0.016
No.1···No.5	H···N	−0.0329	−0.0324	0.1375	0.0207	0.0722	0.016
No.5···No.4	H···O	−0.0214	−0.0211	0.1170	0.0289	0.0745	0.014

All λ_i, $\rho_b(\mathbf{r}_{cp})$, $\nabla^2_\rho(\mathbf{r}_{CP})$ values in atomic unit. See Fig. 2 for details.

2.2. Atoms in molecules (AIM) calculations

AIM analyses were performed using AIM 2000 code [34]. The bonding patterns of sulfamerazine and sulfathiazole clusters can be reliably obtained from detailed analysis of electron density via its topographical study. In this analysis, bond critical points, BCPs, of electron density distribution (points where $\bigtriangledown\rho = 0$ and $\bigtriangledown(\bigtriangledown^2\rho) = 0$) are obtained and additional characterization is done using the corresponding Hessian matrix (a 3×3 matrix of second derivatives). Diagonalization of this matrix yields the coordinate invariant eigenvalues: $\lambda_1 \leq \lambda_2 \leq \lambda_3$ .The Laplacian of charge density at the BCP, $\bigtriangledown^2\rho_b$, and ellipticity, ε, quantities are defined as:

$$\nabla^2\rho_b = \sum_{i=1}^{3}\lambda_i$$

$$\varepsilon = \frac{\lambda_1}{\lambda_2} - 1$$

Negative values for Laplacian indicate presence of covalent bond, whereas positive values reveal non-covalent interactions. Ellipticity is a measure of bond stability; high ellipticity values indicate instability of the bond [35].

3. Results and discussion

In the present work, H-bonding effects on the ^{14}N EFG tensors of crystalline sulfamerazine and sulfathiazole are taken into con-

sideration. As in Figs. 1 and 2, various intermolecular hydrogen bonds are present in solid sulfamerazine and sulfathiazole. Different H-bonding effects on the EFG tensors at the sites of nitrogens can be inferred by a quick look at the results. Furthermore, EFG calculations indicate that the parameters calculated via 6-311++G(d,p) and 6-311+G(d) basis sets are practically coincident with each other. In the following sections, the ^{14}N EFG calculations and AIM analyses based on B3LYP/6-311++G(d,p) will be discussed separately for sulfamerazine and sulfathiazole.

3.1. EFG calculations

3.1.1. Sulfamerazine

The different polymorphs of sulfamerazine are discussed in Ref. [18]. The sulfamerazine molecules can exist in different conformations as a result of rotation across the C–S, S–N and N–C bonds. Polymorph *I* of sulfamerazine is monoclinic [18] with the space group $P2_1/c$ with a = 11.09 Å, b = 8.32 Å, c = 13.96 Å, β = 99.33° and four formula units per unit cell. The two six membered rings are approximately planar and dihedral angle between the planes through the benzene ring and the pyrimidine ring is 64.39°. The crystal structure of sulfamerazine is stabilized by various intermolecular N–H···N and N–H···O hydrogen bonds (Fig. 1), which result in the formation of a hydrogen-bonded network.

In crystalline sulfamerazine, the target molecule forms four hydrogen bonds with the neighbors (Fig. 1). As Table 1 presents, H-bonding interactions have a significant influence on the calculated ^{14}N EFG tensors. As a general trend, ^{14}N quadrupole coupling constants reduce from the monomer to the target molecule in the cluster. It is also found that H-bonding interactions have different influences on ^{14}N quadrupole coupling tensor eigenvalues. N1, with 1.50 MHz reduction in QCC(N1) parameter, is the most affected nucleus in sulfamerazine. Besides, changes in other principal components and asymmetry parameter of N1 are remarkable: $\Delta\chi_{xx}$ = 1.18 MHz, $\Delta\chi_{yy}$ = 0.68 MHz and $\Delta\eta_Q$ = 0.43. The results suggest that the H-bonding interactions at N1 site of crystalline sulfamerazine are rather strong: $\mathbf{r}_{[N1-H\cdots O]}$ = 1.81 Å. For the quadrupole coupling tensor at N2 site, the comparison of isolated gas-phase model and tetrameric cluster shows some discrepancy, although not as dramatic as the N1. By a quick look at the Fig. 1, H-bonding interaction is detected between N2 atom of the target molecule and molecule No.4, which is located in the adjacent parallel layer. Having a proper intermolecular N···O distance, $\mathbf{r}_{N2-H\cdots O}$ = 1.93 Å, 0.54 MHz reduction in QCC(N2) and 0.24 units increase in η_Q(N2) is evidenced, depending on whether the sulfamerazine is in an isolated gas-phase or H-bonded network. N3, in the target molecule, interacts with N1, in molecule No.2, forming a bond with $\mathbf{r}_{[N3\cdots H-N]}$ = 1.81 Å. For this nucleus, QCC(N3) undergoes 0.48 MHz reduction from the monomer to the target molecule in the cluster. On the other hand, in contrast to the N1, N2 and N3 nuclei, the quadrupole coupling tensor at the N4 site shows a negligible sensitivity to H-bonding interactions. From the monomer to the target molecule in the cluster, QCC(N4) and η_Q(N4) values reduce only by 0.19 and 0.09 MHz, respectively. This is due to the limited involvement of this nucleus in the intermolecular interactions of solid sulfamerazine. The overall good agreement between the calculated ^{14}N quadrupole coupling tensors and experimental data is shown in Fig. 3.

Finally, it is worth noting that in addition to the principal eigenvalues of the quadrupole coupling tensor, theoretical calculations provide information on the orientation of quadrupole coupling components in the molecular frame of reference. As in Fig. 4, χ_{zz} component of N1 atom tends to orientate normally to the N–H bond, whereas both χ_{xx} and χ_{yy} are approximately in N–H···N hydrogen bond plane and produce 16.80 and 73.20° angles with N–H bond direction, respectively. However, for the N2 site, both χ_{xx} and χ_{yy} components lie in the amine plane and χ_{zz} orientates along the norm of the plane.

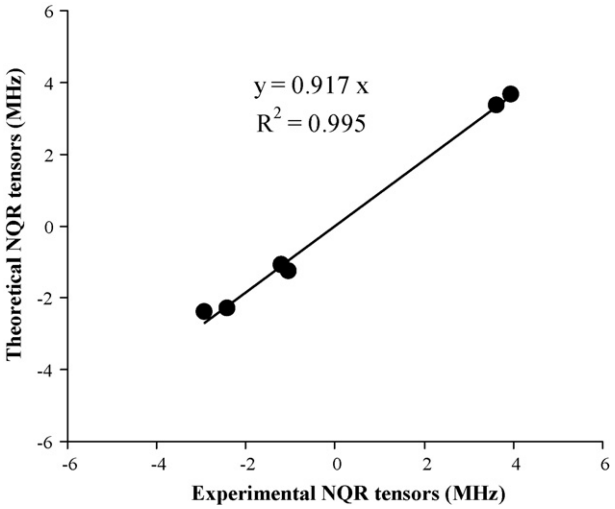

Fig. 3. Correlation of theoretical NQR parameters (at the B3LYP/6-311++G** level) with experimental data in sulfamerazine.

3.1.2. Sulfathiazole

Sulfathiazole crystallizes in the monoclinic space group $P2_1/n$ with a = 10.40 Å, b = 15.13 Å and c = 14.28 Å, β = 91.21° and eight molecular units per unit cell [32]. The six and five membered rings are approximately planar and dihedral angle between the planes

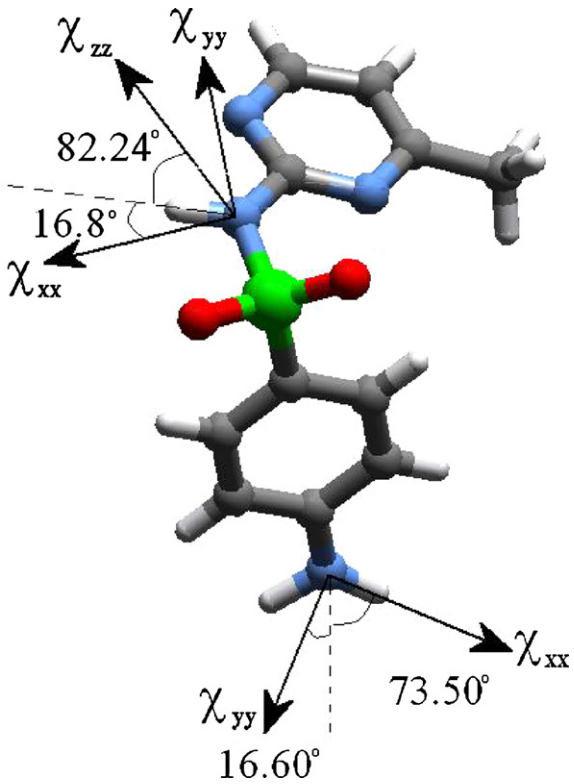

Fig. 4. Orientation of nuclear quadrupole coupling components in molecular frame axes for crystalline sulfamerazine (The component not represented is perpendicular to the molecular plane).

through the benzene ring and the pyrimidine ring is 60.45°. Compared to the crystalline sulfamerazine, NH_2 group is capable of contributing to both N–H···O and N–H···N hydrogen bonds in the crystalline sulfathiazole. These O and N nuclei belong to the adjacent molecules (No. 4 and 5) with $\mathbf{r}_{[N3-H\cdots O]}$ = 1.93 Å and $\mathbf{r}_{[N3-H\cdots N]}$ = 1.94 Å, respectively. Furthermore, the following trends are detected for sulfamerazine and sulfathiazole: First, the N–H···O distance is approximately similar for the two molecules. Second, the EFG tensor at sulfathiazole N2 is more influenced compared to that of sulfamerazine: Δ(QCC(N2)) = 2 MHz and $\Delta\eta_Q$ = 0.22, which reveals the greater H-bonding effects on EFG(N2) tensor. Third, since the chemical environment and charge distribution of the two amine sites are different, the QCC(N2) value for sulfathiazole is in the lower-field. These trends reveal the significant role of $-NH_2$ group in strong hydrogen-bonding interactions of crystalline sulfathiazole.

Fig. 2 shows that N1 of the target molecule is involved in N···H–N H-bonding interaction with $-NH_2$ group of adjacent anti-parallel layer (molecule No. 3). According to the calculations, the interaction can influence EFG tensors at the two nitrogen sites. However, besides the nature of interaction (proton donor versus proton acceptor), the $\mathbf{r}_{[N-H\cdots N]}$ distance of the crystalline sulfathiazole is about 0.13 Å longer than that of sulfamerazine. Therefore, QCC(N1) reduces by 0.44 MHz from the monomer to the target molecule in pentamer cluster. Regarding the data presented in Table 2, the following results are derived by comparing the N3 site of sulfathiazole with sulfamerazine: First, N3–H···O interaction in sulfathiazole is replaced by N3···H–N type in sulfamerazine, which is mostly responsible for the variation of EFG(N3) tensors. Second, presence of the sulfur atom in sulfathiazole may also create different local environment and field gradient at the N3 site. Third, N3 nucleus of sulfathiazole is placed in a five-membered ring. These trends are in agreement with the results of Tables 1 and 2 where QCC(N3) of sulfathiazole is smaller by 1.25 MHz than sulfamerazine. Comparison of the calculated ^{14}N NQR parameters of sulfathazine with available experimental data also shows an acceptable compatibility between the theoretical and experimental parameters with slope = 0.972 and R^2 = 0.999 (Fig. 5).

The obtained results for ^{14}N quadrupole coupling tensors of crystalline sulfathiazole reveal that orientation of χ_{ii} components at the N1 and N2 sites is completely different from those of sulfamerazine (Fig. 6). For the N1 site of sulfathiazole, the χ_{xx} component is tilted 55.1° from N···H–N

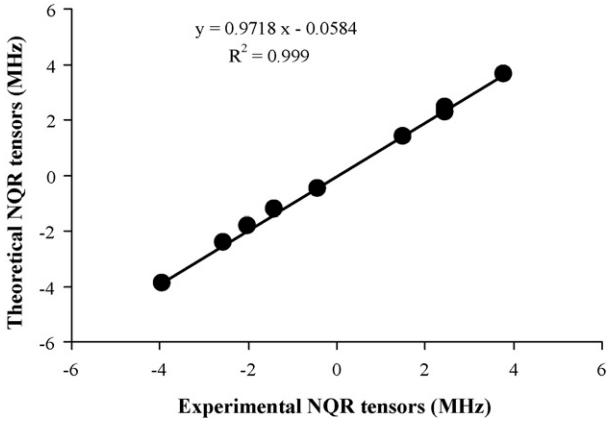

Fig. 5. Correlation of theoretical NQR parameters (at the B3LYP/6-311++G** level) with experimental data in sulfathiazole.

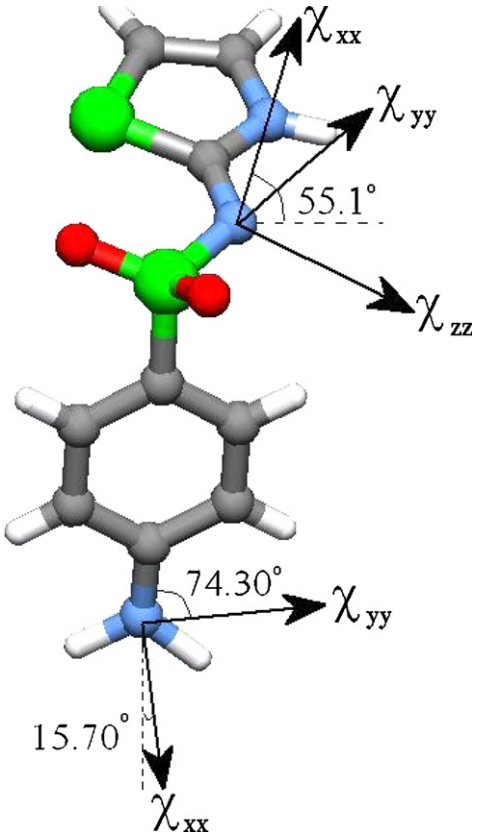

Fig. 6. Orientation of nuclear quadrupole coupling components in molecular frame axes for crystalline sulfathiazole. (The component not represented is perpendicular to the molecular plane).

bond, but the χ_{yy} and χ_{zz} components lie in the plane of the five-member ring. However, at the N2 site, the χ_{zz} orientation is almost perpendicular to the amine site and both χ_{xx} and χ_{yy} components lie in the plane.

3.2. AIM analysis

The AIM theory is applied here to analyze the characteristics of the H···N and H···O bond critical points. Based on the AIM theory, properties of BCP may be applied to summarize the nature of interaction between two atoms as shared (covalent) or closed-shell (ionic). The value of ρ at a BCP, $\rho_b(\mathbf{r}_{cp})$, serves as a measurement for bond strength. Bader found a linear relationship between electron charge density value at hydrogen BCP with hydrogen bond strength and length [35].

Tables 3 and 4 give λ_i, $\rho_b(\mathbf{r}_{cp})$, $\nabla^2_\rho(\mathbf{r}_{CP})$ and ε values at H···N as well as H···O BCPs for sulfamerazine and sulfathiazole, respectively. In accordance with the previous studies [35], the positive $\nabla^2_\rho(\mathbf{r}_{cp})$ value has the same order of magnitude as $\rho(\mathbf{r}_{cp})$ ($\sim 10^{-2}$ au), indicating that the intermolecular N–H···O and N–H···N interactions have the general characteristics of the hydrogen bond. For crystalline sulfamerazine, the $\rho_b(\mathbf{r}_{cp})$ and Laplacian of charge density, $\nabla^2_\rho(\mathbf{r}_{cp})$, at N–H···N and N–H···O BCPs are all in the proposed ranges of 0.0145–0.0344 au and 0.0909–0.1011 au, respectively. On the other hand, the estimated values of $\rho_b(\mathbf{r}_{cp})$ for H-bonding interactions of central sulfathiazole with its neighbors are 0.0291, 0.0192, 0.0217, 0.0199, 0.0207, 0.0289 au (Table 4). As a trend, the value of $\rho_b(\mathbf{r}_{cp})$ for N–H···N interaction in crystalline sulfamerazine is 1.29 times of the sulfathiazole. According to quadrupole coupling constants of donor nitrogens and $\rho_b(\mathbf{r}_{cp})$ values in ^{14}N–H···N and ^{14}N–H···O interactions, an

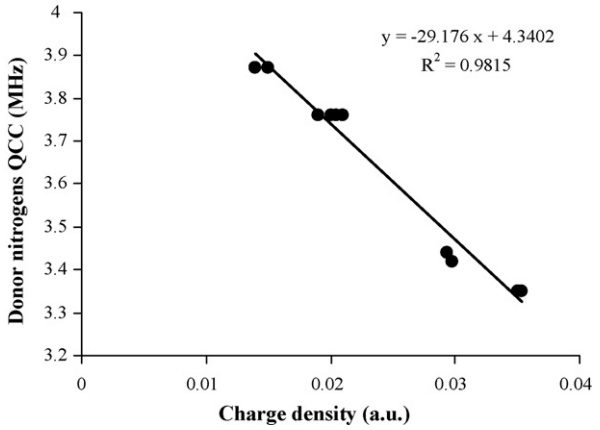

Fig. 7. Correlation of calculated donor nitrogen QCCs with charge density at N–H···O and N–H···N BCPs of sulfamerazine and sulfathiazole.

acceptable linear relation between the two physical quantities is observed (Fig. 7):

$$\mathrm{QCC(MHz)} = -29.176\rho_b(\mathbf{r}_{CP}) + 4.3402 \quad (R^2 = 0.9815)$$

This correlation indicates that the two representations of hydrogen bond properties, based upon NQR and AIM, are approximately equivalent. It is also possible to compare the strength of hydrogen bonds in the two sulfa drugs. In agreement to the calculated NQR parameters, the N–H···N hydrogen bond between target molecule and molecule No. 2 in sulfamerazine is more stable than N–H···O interaction in sulfathiazole. This is due to smaller $\rho_b(\mathbf{r}_{cp})$ as well as larger ellipticity value for the latter case. The ellipticity for N(2)–H···O interaction (target molecule and No. 4) in sulfamerazine is about 1.6 times greater than the value calculated for sulfathiazole. These reveal, in agreement with the previous section, different contributions of nitrogen atoms in formation of H-bonding interactions in the crystalline sulfamerazine and sulfathiazole.

4. Conclusion

DFT investigation of the ^{14}N quadrupole coupling tensors as well as AIM analysis study was performed for sulfamerazine and sulfathiazole in their crystalline phases. According to the results, it is concluded that the ^{14}N quadrupole coupling components and their relative orientations are appropriate to characterize the properties of H-bonding interactions in solid-phase. Besides, calculated NQR parameters change via H-bonding interactions within the two molecular structures. Considering the available experimental and theoretical errors in determination of NQR parameters, the calculated χ_{ii} and η_Q values of ^{14}N nuclei are consistent with experimental values. Investigation of crystalline sulfamerazine and sulfathiazole also reveals the important role of nitrogen nuclei in formation of H-bonding interactions in solid-phases. According to QCC of donor nitrogens and $\rho_b(\mathbf{r}_{cp})$ values in N–H···N and N–H···O interactions, an acceptable linear relation between the two physical quantities is observed.

References

[1] A.V. Finkelstein, O.B. Ptitsyn, Protein Physics, Academic Press, London, 2002.
[2] R. Bersohn, Nuclear electric quadrupole spectra in solids, J. Chem. Phys. 20 (1952) 1505–1509.
[3] E.A.C. Lucken, Nuclear Quadrupole Coupling Constants, Academic Press, London, 1992.
[4] B. Nogaj, Hydrogen-bond theories and models based on nuclear quadrupole resonance spectroscopy studies, J. Phys. Chem. 91 (1987) 5863–5869.
[5] M. Cotten, V.G. Soghomonian, W. Hu, T.A. Cross, High resolution and high fields in biological solid state NMR, Solid State NMR 9 (1997) 77–80.
[6] A. Watts, I.J. Burnett, C. Glaubitz, G. Gröbner, D.A. Middleton, P.J.R. Spooner, J.A. Watts, P.T.F. Williamson, Membrane protein structure determination by solid state NMR, Nat. Prod. Rep. 16 (1999) 419–423.
[7] J. Seliger, V. Zagar, A. Zidansek, R. Blinc, N-14 nuclear quadrupole resonance of picolinic, nicotinic, isonicotinic and dinicotinic acids, Chem. Phys. 331 (2006) 131–136.
[8] G. Wu, S. Dong, R. Ida, N. Reen, A solid-state ^{17}O nuclear magnetic resonance study of nucleic acid bases, J. Am. Chem. Soc. 124 (2002) 1768–1777.
[9] B. Zhou, T. Giavani, H. Bildsøe, J. Skibsted, H.J. Jakobsen, Structure refinement of CsNO3(II) by coupling of ^{14}N MAS NMR experiments with WIEN2k DFT calculations, Chem. Phys. Lett. 402 (2005) 133–137.
[10] M.J. Duer, Solid State NMR Spectroscopy, Blackwell Science Ltd., London, 2002.
[11] T.H. Maren, Relations between structure and biological activity of sulfonamides, Annu. Rev. Pharmacol. 16 (1976) 309–327.
[12] R.J. Mesley, E.E. Houghton, Infrared identification of pharmaceutically important sulfonamides with particular reference to the occurrence of polymorphism, J. Pharm. Pharmacol. 19 (1967) 295–304.
[13] S.S. Yang, J.K. Guillory, Polymorphism in sulfonamides, J. Pharm. Sci. 61 (1972) 26–40.
[14] Y. Funahashi, N.H. Sugi, T. Semba, Y. Yamamonoto, S. Hamaoka, N.T. Tamai, Y. Ozawa, A. Tsuruoka, K. Nara, K. Takahashi, T. Kabe, J. Kamata, T. Owa, N. Veda, T. Haneda, M. Yonega, K. Yoshimatsu, T. Wakabayashi, Sulfonamide derivative, E7820, is a unique angiogenesis inhibitor suppressing an expression of integrin alpha 2 subunit on endothelium, Cancer Res. 62 (2002) 6116–6123.
[15] T. Semba, Y. Funahashi, N. Ona, Y. Yamamoto, N.H. Sugi, M. Asada, K. Yoshimatsu, T. Wakabayashi, An angiogenesis inhibitor E7820 shows broad-spectrum tumor growth inhibition in a xenograft model: possible value of integrin alpha 2 on platelets as a biological marker, Clin. Cancer Res. 10 (2004) 1430–1438.
[16] J. Slawinski, M. Gdaniec, Synthesis, molecular structure, and in vitro antitumor activity of new 4-chloro-2-mercaptobenzenesulfonamide derivatives, European J. Med. Chem. 40 (2005) 377–389.
[17] Q. Chen, P.N.P. Rao, E.E. Knaus, Design, synthesis, and biological evaluation of linear 1-(4-, 3- or 2-methylsulfonylphenyl)-2-phenylacetylenes: A novel class of cyclooxygenase-2 inhibitors, Bioorg. Med. Chem. 13 (2005) 2459–2468.
[18] G.M.G. Hossain, A new polymorph of sulfamerazine, Acta Crystallogr. E 62 (2006) 2166–2167.
[19] K.R. Acharya, K.N. Kuchela, G. Kartha, Crystal structure of sulfamerazine, J. Crystallogr. Spectrosc. Res. 12 (1982) 369–376.
[20] X. Cao, C. Sun, T.J. Thamann, A study of sulfamerazine single crystals using atomic force microscopy, transmission light microscopy, and Raman spectroscopy, J. Pharm. Sci. 94 (2005) 1881–1892.
[21] M.R. Caira, R. Mohamed, Positive indentification of two orthorhombic polymorphs of sulfamerazine ($C_{11}H_{12}N_4O_2S$), their thermal analyses and structural comparison, Acta Crystallogr. B 48 (1992) 492–498.
[22] R. Blinc, T. Apih, J. Seliger, Nuclear quadrupole double resonance techniques for the detection of explosives and drugs, Appl. Magn. Reson. 25 (2004) 523–534.
[23] J. Seliger, V. Zagar, R. Blinc, A new highly sensitive ^{1}H-^{14}N nuclear-quadrupole double resonance technique, J. Magn. Reson., Ser A 106 (1994) 214–222.
[24] C. Sun, D.J.W. Grant, Influence of crystal structure on the tabulating properties of sulfamerazine polymorphs, Pharm. Res. 18 (2001) 274–280.
[25] D.A. Adsmond, D.J.W. Grant, Hydrogen bonding in sulfonamides, J. Pharm. Sci. 90 (2001) 2058–2077.
[26] R. Blinc, J. Seliger, A. Zidansek, V. Zagar, F. Milia, H. Robert, N-14 nuclear quadrupole resonance of some sulfa drugs, Solid State Nucl. Magn. Reson. 30 (2006) 61–68.
[27] F. Elmi, N.L. Hadipour, A study on the intermolecular hydrogen bonds of α-glycylglycine in its actual crystalline phase using ab initio calculated ^{14}N and ^{2}H nuclear quadrupole coupling constants, J. Phys. Chem. A 109 (2005) 1729–1733.
[28] R. Ida, M.D. Clerk, G. Wu, Influence of N–H···O and C–H···O hydrogen bonds on the ^{17}O NMR tensors in crystalline uracil: computational study, J. Phys. Chem. A 110 (2006) 1065–1071.
[29] M.J. Frisch, G.W. Trucks, H.B. Schlegel, G.E. Scuseria, M.A. Robb, J.R. Cheeseman, V.G. Zakrzewski, J.A. Montgomery, R.E. Stratmann, J.C. Burant, S. Dapprich, J.M. Millam, A.D. Daniels, K.N. Kudin, M.C. Strain, O. Farkas, J. Tomasi, V. Barone, M. Cossi, R. Cammi, B. Mennucci, C. Pomelli, C. Adamo, S. Clifford, J. Ochterski, G.A. Petersson, P.Y. Ayala, Q. Cui, K. Morokuma, D.K. Malick, A.D. Rabuck, K. Raghavachari, J.B. Foresman, J. Cioslowski, J.V. Ortiz, B.B. Stefanov, G. Liu, A. Liashenko, P. Piskorz, I. Komaromi, R. Gomperts, R.L. Martin, D.J. Fox, T. Keith, M.A. Al-Laham, C.Y. Peng, A. Nanayakkara, C. Gonzalez, M. Challacombe, P.M.W. Gill, B. Johnson, W. Chen, M.W. Wong, J.L. Andres, M. Head-Gordon, E.S. Replogle, J.A. Pople, Gaussian 98, revision A.6, Gaussian, Inc., Pittsburgh, PA, 1998.
[30] A.D. Becke, Density-functional exchange-energy approximation with correct asymptotic behavior, Phys. Rev. A 38 (1988) 3098.
[31] C. Lee, W. Yang, R.G. Parr, Development of the Colle-Salvetti correlation-energy formula into a functional of the electron density, Phys. Rev. B 37 (1988) 785.
[32] M.B. Hursthouse, A new polymorph of sulfathiazole, Acta Cryst. C 55 (1999) 1831–1833.
[33] P. Pyykkö, Spectroscopic nuclear quadrupole moment, Mol. Phys. 99 (2001) 1617–1629.
[34] F. Biegler-Konig, J. Schonbohm, D. Bayles, Software news and updates – AIM2000 – A program to analyze and visualize atoms in molecules, J. Comput. Chem. 22 (2001) 545–559.
[35] R.F.W. Bader, Atoms In Molecules—A Quantum Theory, Oxford University Press, New York, 1990.